

## A vacuole localized $\beta$ -glucosidase contributes to drought tolerance in *Arabidopsis*

WANG PengTao, LIU Hao, HUA HongJie, WANG Lei & SONG Chun-Peng\*

State Key Laboratory of Cotton Biology, Laboratory of Plant Stress Biology, Department of Biology, Henan University, Kaifeng 475004, China

Received July 21, 2011; accepted September 1, 2011

The phytohormone abscisic acid (ABA) plays a critical role in plant growth, development, and adaptation to various stress conditions. The cellular ABA level is constantly adjusted to respond to changing physiological and environmental conditions. To date, the mechanisms for fine-tuning ABA levels remain elusive. Here, we report that BGLU10, a member of a multigene family of  $\beta$ -glucosidases, contributes to drought tolerance in *Arabidopsis*. The T-DNA insertion mutant *bglu10* exhibited a drought-sensitive phenotype, characterized by an increased rate of water loss, and lower leaf temperature,  $\beta$ -glucosidase activity, ABA content, and expressions of ABA- and drought-responsive genes under drought stress. In contrast, lines overexpressing *BGLU10* showed greater drought resistance than that of the wild-type, as shown by decreased water loss via transpiration, higher  $\beta$ -glucosidase activity, ABA level, and expressions of ABA- and stress-responsive genes under drought stress. Transient expression of BGLU10::GFP and  $\gamma$ -TIP1::RFP in mesophyll cell protoplasts showed that the BGLU10 enzyme protein was localized to the vacuole. Meanwhile, *BGLU10* was expressed in various organs, and was induced by several abiotic stresses, suggesting that BGLU10 may be involved in a variety of stress responses, and that hydrolysis of ABA-GE produces free ABA in the plant stress response.

***Arabidopsis*,  $\beta$ -glucosidase, BGLU10, ABA, drought**

**Citation:** Wang P T, Liu H, Hua H J, et al. A vacuole localized  $\beta$ -glucosidase contributes to drought tolerance in *Arabidopsis*. Chinese Sci Bull, 2011, 56: 3538–3546, doi: 10.1007/s11434-011-4802-7

The plant hormone abscisic acid (ABA) plays a crucial role in plant responses to several abiotic stresses such as drought, salt, and cold. It also plays roles in plant growth and development, including seed dormancy, germination, seedling growth, lateral root development, transition from the vegetative to the reproductive phase, and senescence [1–3]. Cellular ABA levels constantly fluctuate allow plants to adapt to the changing physiological and environmental conditions. In particular, there are dramatic increases in the cellular level of ABA during seed maturation and under abiotic stresses, while there is a distinct decrease in the ABA level during seed germination [4,5].

The cellular ABA level is controlled by complex *de novo* synthesis pathways, and hydroxylation and conjugation reactions. The *de novo* synthesis pathway is now well charac-

terized in plants, especially in *Arabidopsis* [6]. All the steps for *de novo* ABA synthesis occur in plastids, except for the final two steps involving the conversion of xanthoxin to ABA, which take place in the cytoplasm [7]. The importance of *de novo* ABA synthesis to increase cellular ABA levels has been well established using biosynthetic mutants with a variety of physiological defects, including precocious germination, wilting, and sensitivity to environmental stresses [8]. A large body of evidence has shown that genes encoding biosynthetic enzymes are upregulated in response to physiological cues or environmental stresses, leading to an increase in *de novo* ABA synthesis [9,10]. On the other hand, ABA is catabolized into inactive forms by either oxidation or conjugation [6]. The oxidative pathways play a pivotal role in various physiological processes. The major oxidative pathway is catalyzed by ABA 8'-hydroxylase, which converts ABA' C-8'-hydroxy to into 8'-

\*Corresponding author (email: songcp@henu.edu.cn)

hydroxy ABA (8'OH-ABA). In the subsequent step, 8'OH-ABA is spontaneously isomerized to form phaseic acid (PA), which is then converted to dihydrophaseic acid (DPA). ABA 8'-hydroxylase is a cytochrome P450 monooxygenase that is induced by ABA and dehydration stress [11]. In addition to 8'OH-ABA, 7'OH-ABA and 9' OH-ABA were also found as minor catabolites in a variety of plant species [6]. As for the conjugation pathway, the carboxyl (at the C-1) and hydroxyl groups of ABA and its oxidative catabolites are potential targets for conjugation with glucose. Among such conjugates, ABA glucose ester (ABA-GE) is the predominant form [12]. An ABA-specific glucosyltransferase catalyzes the conjugation process [13]. The conventional view of ABA-GE, which accumulates in plant vacuoles or apoplastic spaces during aging and stress treatments [14], is that it is a physiologically inactive end-product of ABA metabolism rather than storage or transport form. However, some other reports have suggested that ABA-GE is a long-distance transport form of the hormone, providing a source of ABA for subsequent hydrolysis [15]. Furthermore, exogenously applied ABA-GE inhibited growth of hypocotyls of *Arabidopsis* seedlings; since ABA-GE cannot migrate passively through the plasma membrane, this result implied that exogenously applied ABA-GE may be absorbed by roots and then hydrolyzed by ABA- $\beta$ -D-glucosidase, liberating free ABA. This could then potentially inhibit the growth of *Arabidopsis* hypocotyls [16]. In 2006, Lee et al. [17] provided direct evidence that ABA-GE can be hydrolyzed in response to stress by the  $\beta$ -glucosidase AtBG1, resulting in an increase in the concentration of active ABA. AtBG1  $\beta$ -glucosidase is located in the endoplasmic reticulum (ER) and remains in the ER during stress responses. As mentioned above, ABA-GE is located in intracellular storage organelles (vacuoles), in xylem sap, and probably in the cell wall as well [18]. Thus, it was proposed that uncharacterized membrane-localized transporter proteins may be involved in the movement of ABA-GE into the ER.

Database searches have revealed a multigene family of  $\beta$ -glucosidases, which has 48 members in *Arabidopsis* [19]. The AtBG1 protein studied by Lee et al. [17] is BGLU18. In the present study, our results showed that BGLU10, another member of the  $\beta$ -glucosidase family in *Arabidopsis*, is localized in vacuoles and played roles in drought tolerance.

## 1 Materials and methods

### 1.1 Plant materials and growth conditions

*Arabidopsis thaliana* ecotype Columbia was used in this study. Seeds were sterilized and kept for 3 d at 4°C in the dark to break dormancy. The seeds were then sown on MS medium containing 0.6% agar and incubated at 22±2°C with a 16-h-light/8-h-dark photoperiod and 70% relative humidity (RH). Seedlings were transferred to soil at 7–10 d after germination and placed in a growth chamber at

(22±2)°C under a 16-h-light/8-h-dark photoperiod and 70% RH, and watered every other day for normal growth conditions. For drought stress conditions, plants were grown under normal watering conditions for 20 d and then stressed by withholding irrigation for 10 d.

### 1.2 Isolation of *bglu10* mutant

The T-DNA insertion lines for *BGLU10* (*At4g27830*) SALK\_101672 were ordered from the *Arabidopsis* Biological Resource Center (ABRC) (<http://www.arabidopsis.org/abrc/>). Homozygous mutant plants were screened by PCR amplification using gene-specific primers LP (TTAACGGTCAAGACAACGACC), RP (ATCCTTTACATGATTTTTCGG) and vector left-border-specific primers LBal (TGGTTCACGTAGTGGGCCATCG) and LBb1 (GCGTGACCGCTTGCTGCAACT). The homozygous lines were backcrossed with wild-type (WT) plants, and the F<sub>2</sub> progeny were used for phenotype analysis.

### 1.3 Plasmid constructs

The gene-specific cDNA fragment of *BGLU10* was amplified by PCR, and the following primer pairs were used to construct the super1300+ over-expression plasmid: forward primer CCCCTGCAGATGAACTTTACTCTCTACTTTCCGTTTTCT and reverse primer CCCGTTCGACATTACAAATGAAGAAGAGCCAGAGATGTTGCTCTG (*Pst*I and *Sal*I restriction sites underlined in forward and reverse primers, respectively). For the subcellular localization of BGLU10, the cDNA for *BGLU10* was amplified by PCR using the following primers: forward CCCGTTCGACATGAACTTTACTCTCTACTTTCCG (*Sal*I site underlined); reverse GGCCCGCGGTCAATGAAGAAGAGCCAGAGATGTTGC (*Sac*II site underlined), digested with *Sal*I and *Sac*II, and inserted into the pHBT-GFP vector. To verify that BGLU10 was localized in the vacuole, a cDNA fragment of  $\gamma$ -*TIP1* (*At2g36830*) as a marker protein for the vacuole was amplified by PCR with the following primers: forward CCCGTTCGACATGCCGATCAGAAACATCGCC (*Sal*I site underlined), reverse GGCGGATCCCGGTAGTCTGTGGTTGGGAGCTG (*Bam*HI site underlined), then digested with *Sal*I and *Bam*HI and inserted into the pHBT-DsRed vector. For the *BGLU10* promoter-GUS construct, an 800-bp *BGLU10* promoter fragment was obtained by PCR using the primer pairs CCCGAATTCCTTATCTTCGATCATCTAAGTTA and GGGCTGCAGTTTGCTTTTGCTACTTTCGTG. The forward primer and reverse primer contained *Eco*RI and *Pst*I restriction sites, respectively (underlined). The promoter fragments were then cloned into pCAMBIA1381 between the *Eco*RI and *Pst*I sites.

### 1.4 Plant transformation and protoplast transfection

The constructs were introduced into *Agrobacterium tumefaciens*

*ciens* strain GV3101 and transformed by floral infiltration into WT *Arabidopsis* (Columbia ecotype) for gene overexpression and GUS staining assays. To observe the subcellular localization of the proteins of interest, protoplasts isolated from *Arabidopsis* leaves were transformed with plasmid combinations BGLU10-pHBT-GFP and  $\gamma$ -TIP1-pHBT-DsRed as described previously [20]. After incubation for 16 to 20 h, the fluorescence of protoplasts was detected under a laser scanning confocal microscope.

### 1.5 Confocal imaging for BGLU10 subcellular localization

The fluorescence of the protoplasts was observed under a laser scanning confocal microscope (FV1000, Olympus, Japan). The protoplasts were excited at 488 nm and fluorescence was detected at 500–530 nm for GFP and 650–750 nm for autofluorescence of chloroplasts. RFP was excited at 543 nm and detected at 560–630 nm, and transmitted fields were collected simultaneously for use in merged images. Magnification at 60 $\times$  using an oil immersion lens was used to obtain high resolution images of cells.

### 1.6 Histochemical detection of GUS activity

Ten independent transgenic lines containing the *BGLU10* promoter-GUS constructs were tested for GUS activity by incubation of excised tissues in GUS staining buffer (3 mmol/L 5-bromo-4-chloro-3-indolylb-glucuronic acid, 0.1 mol/L sodium phosphate buffer, pH 7.0, 0.1% Triton X-100, and 8 mmol/L  $\beta$ -mercaptoethanol) at 37 $^{\circ}$ C in the dark overnight. The staining was terminated by replacement of the staining solution with 70% ethanol solution, and samples were stored at 4 $^{\circ}$ C until microscopic observations.

### 1.7 Semi-quantitative RT-PCR and real-time quantitative RT-PCR

Plants were grown in chamber for 15 d at 22 $\pm$ 2 $^{\circ}$ C under a 16-h-light/8-h-dark photoperiod and 70% RH, and watered every other day for normal growth conditions as control. For drought stress treatments, plants were grown under normal watering conditions for 10 d and then stressed by completely withholding irrigation for 5 d. Total RNA was isolated from 100 mg tissue samples using TRIZOL reagent (Invitrogen, USA). First strand cDNA was synthesized using Maloney murine leukemia virus (MMLV) reverse transcriptase (Promega, USA). For semi-quantitative RT-PCR, the volume of each cDNA sample was adjusted to give the same signal strength for *Actin2* after 20 cycles of PCR. The RT-PCR products were analyzed by electrophoresis on 1.5% agarose gels. SYBR Premix Ex Taq (TaKaRa, Japan) and a Stratagene MX3005P (Agilent, USA) apparatus were used for real-time RT-PCR. The cycling conditions were as follows: 30 s at 95 $^{\circ}$ C; 40 cycles of 25 s at 95 $^{\circ}$ C, 25 s at

60 $^{\circ}$ C, and 25 s at 72 $^{\circ}$ C. This was followed by a melting-curve program (60 s at 95 $^{\circ}$ C; 30 s at 55 $^{\circ}$ C; 30 s at 95 $^{\circ}$ C). Specific cDNA was quantified with a standard curve based on known amounts of amplified target gene fragments. The mean value of three replicates was normalized against *Actin2* as the internal control. Real-time quantitative PCR experiments were repeated three times.

### 1.8 Infrared thermography imaging

Thermal imaging of drought-stressed plantlets was performed as described previously [21]. Briefly, plantlets were first grown under well-watered conditions (22 $\pm$ 2 $^{\circ}$ C, 60%–70% RH, 16 h photoperiod, plants watered every other day). Drought stress then was initiated by withholding water for 3 d. Thermal images were obtained within the growth chamber (22 $\pm$ 2 $^{\circ}$ C, 60%–70% RH, 16 h photoperiod) using a ThermaCAM SC3000 infrared camera (FLIR System, USA). Images were analyzed using version 5.31 of the public domain image-analysis program IRWinReport.

### 1.9 Determination of $\beta$ -glucosidase activity

Plants of the WT, *bglu10*, and *BGLU10-OE* lines were grown under normal watering conditions for 20 d or stressed by withholding water for 10 d. Then, plant tissue (2 g) of each type of plants was ground in 100 mL 0.1 mol/L (pH 6.6) phosphate buffered saline before centrifugation at 6000 $\times$ g for 10 min. The supernatant was then adjusted to pH 5.0 with 0.1 mol/L HCl. The homogenate were centrifuged at 6000 $\times$ g for 10 min, and supernatant stored at 4 $^{\circ}$ C before use (within 24 h).

$\beta$ -glucosidase activity was measured by the release of *p*-nitrophenol from the substrate *p*-nitrophenyl- $\beta$ -D-glucopyranoside as described previously [18]. The standard enzyme assay contained 400  $\mu$ L 100 mmol/L citrate buffer adjusted to pH 4.8 with KOH. The stock solution consisted of *p*-nitrophenyl- $\beta$ -D-glucopyranoside dissolved in dimethylformamide (200 mg/mL). For assays, 10  $\mu$ L substrate stock solution and usually 12.5  $\mu$ L enzyme solution were added to the buffer. After 1 h of incubation at 37 $^{\circ}$ C, the reaction was terminated by addition of 1 mL 200 mmol/L Na<sub>2</sub>CO<sub>3</sub> solution. The amount of liberated *p*-nitrophenol was quantified spectrophotometrically at 405 nm using the molar extinction coefficient,  $\epsilon=18300 \Delta\text{Abs}\times 1\times (\text{mol cm})^{-1}$ .

### 1.10 Measurement of endogenous ABA by gas chromatography-mass spectrometry

The level of endogenous ABA was quantified by gas chromatography-mass spectrometry (GC-MS) as described previously [22–26]. Plants were immediately frozen in liquid nitrogen. Frozen samples were lyophilized and stored at –70 $^{\circ}$ C until extraction. Plant samples were extracted with 30 mL of extraction solution (95% isopropanol: 5% glacial

acetic acid). The filtrate was concentrated using a rotary evaporator. The residue was dissolved in 4 mL 1 mol/L NaOH solution, and then washed 3 times with 3 mL methylene chloride to remove lipophilic materials. The aqueous phase was brought to approximately pH 3.5 with 6 mol/L HCl and partitioned three times into EtOAc. EtOAc extracts were then combined and evaporated. The dried residue was dissolved in phosphate buffer (pH 8.0) and then run through a polyvinylpyrrolidone (PVPP) column. The extracts were dried and methylated by adding diazomethane for GC-MS analysis on a 6890N Network GC system, equipped with a 5973 Network Mass Selective Detector (Agilent). The amount of endogenous ABA was calculated by the dividing the endogenous peak area by the internal standard peak area multiplied by amount of internal standard divided by weight.

## 2 Results

### 2.1 Deficiency of *BGLU10* results in drought-sensitive of *Arabidopsis*

In 2006, Lee et al. [17] were the first to show that the cleavage of glucose-conjugated ABA by an ABA-specific  $\beta$ -glucosidase, AtBG1, produced bioactive ABA in response to dehydration stress. *BGLU10*, which was studied in this work, belongs to the multigene family of  $\beta$ -glucosidases in *Arabidopsis* [19]. To examine the role of *BGLU10* in the response of plants to drought stress, we identified a mutant *Arabidopsis* line, *bglu10*, from the SALK collection [27], donor stock number SALK\_101672. This mutant contains a T-DNA insertion in the *BGLU10* gene (At4g27830). The T-DNA is inserted in the third exon of *BGLU10* (Figure 1(a)). The insertion was expected to eliminate or strongly reduce the transcription of *BGLU10*, and this was confirmed by reverse transcriptase-PCR (RT-PCR) analyses (Figure 1(b)). As shown in Figure 1(c), there were no obvious differences between the mutant *bglu10* and the WT when grown under normal watering conditions (16-h-light/8-h-dark photoperiod, 70% RH and watered every other day), but *bglu10* was more sensitive than the WT to drought stress when irrigation was withheld (Figure 1(d)). At 10 d of drought treatment, the WT plants showed slight wilting, whereas the *bglu10* plants were severely wilted or dead. Correspondingly, the leaf temperature of *bglu10* plantlets was 0.6°C lower than that of the WT under drought treatment, as recorded by infrared thermography (Figure 1(e) and (g), significant difference according to the Steel-Dwass test;  $P < 0.05$ ). We then compared the rates of water loss from rosette leaves. The *bglu10* mutant leaves lost water slightly faster than did WT leaves. At 200 min after leaves were cut, leaves of *bglu10* and WT plants had lost water by 38% and 29%, respectively, of their initial moisture (Figure 1(h), significant difference according to the Steel-Dwass test;  $P < 0.05$ ). These temperature differences may reflect the

role of *BGLU10* in the regulation of the ABA content and the stomatal aperture to control transpirational water loss. These results imply that *BGLU10*, like AtBG1, might also contribute to drought tolerance in *Arabidopsis*.

### 2.2 Enhanced drought tolerance in plants overexpressing *BGLU10*

Plants typically synthesize ABA in response to drought. The ABA triggers the closing of stomata, reducing water loss and enhancing drought resistance [28]. To further test whether *BGLU10* might be involved in plant drought stress responses, we generated *BGLU10-OE* lines in which the *BGLU10* gene was upregulated by almost 30 times compared with its expression in the WT (Figure 2(a)). The *bglu10* mutant, overexpression lines, and WT plants were grown in soil for 10 d under normal watering conditions, before drought stress was imposed by withholding irrigation for 5 d. In response to the drought treatment, the mutant plants began to display visible symptoms of dehydration, and WT plants also displayed dehydration symptoms with only temporary wilting. In contrast, *BGLU10-OE* lines showed more normal growth than the WT (Figure 2(b)). Moreover, when the *bglu10* mutant, *BGLU10-OE* lines, and WT plants were rewatered, all leaves of the *BGLU10-OE* lines recovered from dehydration symptoms, whereas the recovery of WT plants was somewhat poorer than that of *BGLU10-OE* lines. In the *bglu10* mutant, only upper leaves were able to recover from dehydration symptoms (Figure 2(c)). Furthermore, the rates of water loss in rosette leaves were consistent with the drought-resistant phenotype (Figure 2(d)). These results implied that the drought tolerance in transgenic plants overexpressing *BGLU10* was increased compared with that of WT plants, and greatly increased compared with that of the mutants.

### 2.3 Contribution of *BGLU10* to drought tolerance

Endogenous ABA levels increase dramatically in response to drought stress in plants, and regulate a complicated gene network system to increase resistance to stresses [9,29]. To further confirm the function of *BGLU10* in drought responses, we examined total  $\beta$ -glucosidase activity under normal growth conditions or drought stress in the *bglu10* mutant, *BGLU10-OE* lines, and WT plants. The total  $\beta$ -glucosidase activity was greater under drought stress conditions than under normal growth conditions in all plants, but in terms of overall activity, the *BGLU10-OE* lines showed the highest activity, and the mutant line *bglu10* showed the lowest (Figure 3(a), significant difference between each pair of lines according to the Steel-Dwass test;  $P < 0.05$ ). Consistent with the results of the  $\beta$ -glucosidase assay, the ABA level showed similar trends under stressed and non-stressed conditions in the *bglu10* mutant, *BGLU10-OE* lines and WT plants (Figure 3(b)). Previous studies

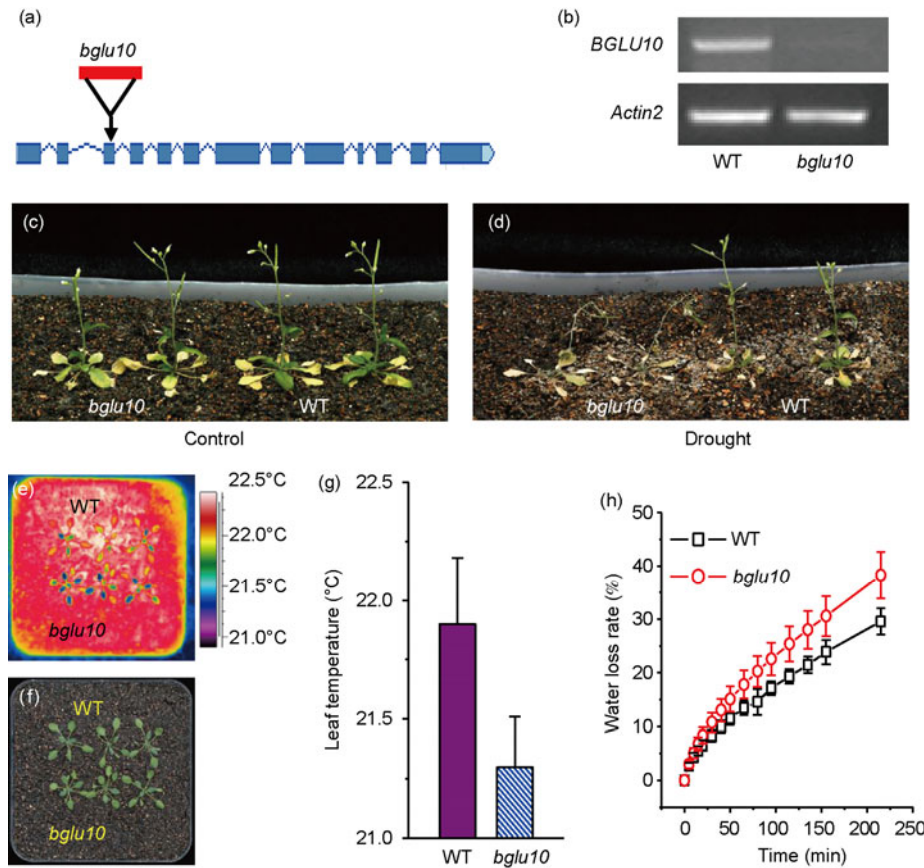


**Figure 1** Deficiency of *BGLU10* results in drought-sensitive plants. (a) Insertion positions of T-DNA in the *BGLU10* gene; (b) reverse transcriptase PCR analysis of *BGLU10* expression. *Actin2* served as the control; (c) plants were grown under normal watering conditions for 30 d after transfer of seedlings to soil at 10 d after germination; (d) plants were grown under normal watering conditions for 20 d, and then stressed by completely withholding water for 10 d; (e) false-color infrared images of drought-stressed plantlets. Thermal images show leaf temperature profiles of 14-d-old WT and *bglu10* plantlets after drought treatment for 3 d; (f) photograph shows seedlings in (e); (g) temperature of the leaf surface in *bglu10* mutant and WT quantified by infrared thermal imaging. Data are means±SD (data are from ~40 measurements of square pixels from each plant, 2 central pixels each leaf); (h) transpirational water loss in WT and *bglu10* lines at indicated time points after detachment. Water loss is shown as a percentage of initial fresh weight (FW). Values are means±SD of 4 samples (each sample had 6 leaves).

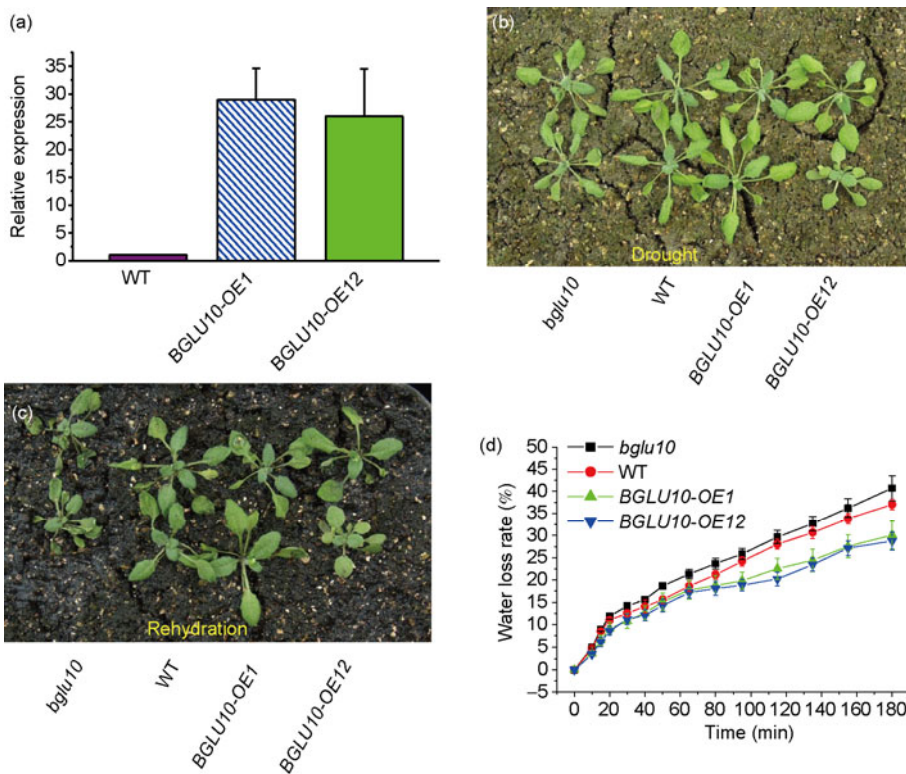


**Figure 2** Enhanced drought stress tolerance in plants overexpressing *BGLU10*. (a) Real-time quantitative PCR analyses of expression levels of *BGLU10* in *BGLU10-OE* and WT plants; (b) dehydration symptoms of *bglu10* mutant, *BGLU10-OE* lines, and WT plants after withholding water for 5 d; (c) recovery of *bglu10* mutant, *BGLU10-OE* lines, and WT plants after rewatering in (b); (d) transpirational water loss in *bglu10* mutant, *BGLU10-OE* lines, and WT plants at indicated time points after detachment. Water loss is expressed as a percentage of initial fresh weight (FW). Values are means±SD of 4 samples (each sample had 6 leaves).

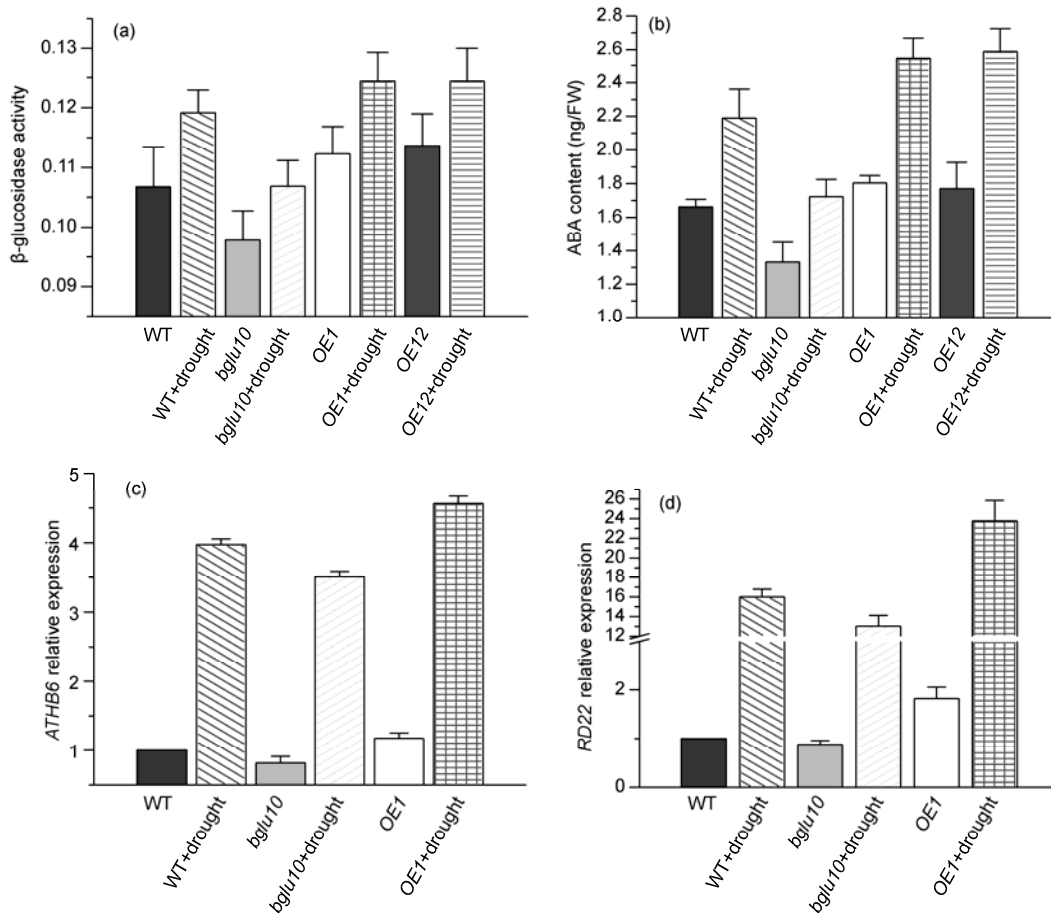


**Figure 3** Contribution of BGLU10 to drought tolerance. (a) Examination of total  $\beta$ -glucosidase activity under normal growth conditions or drought stress in *bglu10* mutant, *BGLU10-OE* lines, and WT plants. Values are means $\pm$ SD of three repeats; (b) ABA content under normal or drought stress conditions in *bglu10* mutant, *BGLU10-OE* lines, and WT plants. Values are means $\pm$ SD of 3 repeats; (c) and (d) real-time quantitative PCR experiments showing expression level of *ATHB6* (ABA response marker gene) and *RD22* (drought response marker gene), respectively, in *bglu10* mutant, *BGLU10-OE*, and WT plants. Values are means $\pm$ SD of 3 repeats.

showed that the expression of *ATHB6* and *RD22* were induced by ABA and drought [30–32]. To determine whether the expressions of ABA- and drought-responsive genes were affected by the *BGLU10* and ABA levels, we used real-time PCR analysis to compare expressions of stress-induced genes among the WT, *BGLU10-OE* lines, and mutants. The results showed that the steady state levels of both *ATHB6* and *RD22* gene transcripts were lower in the mutant than in the WT, whereas greater expressions were observed in *BGLU10-OE* lines than in WT and *bglu10* (Figure 3 (c) and (d)). These findings suggest that BGLU10 may have a general role in regulating the ABA content and ABA-mediated stress gene expression in plants.

#### 2.4 BGLU10 is localized in the vacuole

Previously, it was predicted that BGLU10 might be localized in vacuole based on the potential signal sequences in the deduced precursor proteins, as determined using SignalP V2.0 [19]. We investigated the subcellular localization of

BGLU10 by transient gene expression analysis in mesophyll protoplasts of *Arabidopsis* with the BGLU10-pHBT-GFP plasmid. The green fluorescence of the BGLU10::GFP fusion protein only appeared in compartments of the protoplast that lacked chloroplasts (Figure 4 (a3)). To further examine whether the localization of BGLU10::GFP is vacuolar or not, a tonoplast intrinsic protein  $\gamma$ -TIP1 was chosen as a fluorescent reporter protein for the vacuole [33], and a  $\gamma$ -TIP1::pHBT-DsRed vector was constructed for use in co-localization imaging analyses. The green fluorescence of the BGLU10::GFP fusion protein tightly co-localized with the red fluorescence of the  $\gamma$ -TIP1::DsRed fusion protein (Figure 4 (b3)–(e3)). Meanwhile, only the green fluorescent protein was localized throughout the cells when the protoplasts were transformed with the pHBT-GFP vector control (Figure 4 (a1)–(d1)). Similarly, only the red fluorescent protein was localized throughout the cells when protoplasts were transformed with the pHBT-DsRed vector control (Figure 4 (a2)–(d2)). This result further indicated that BGLU10 is localized in the vacuole. This pattern of locali-



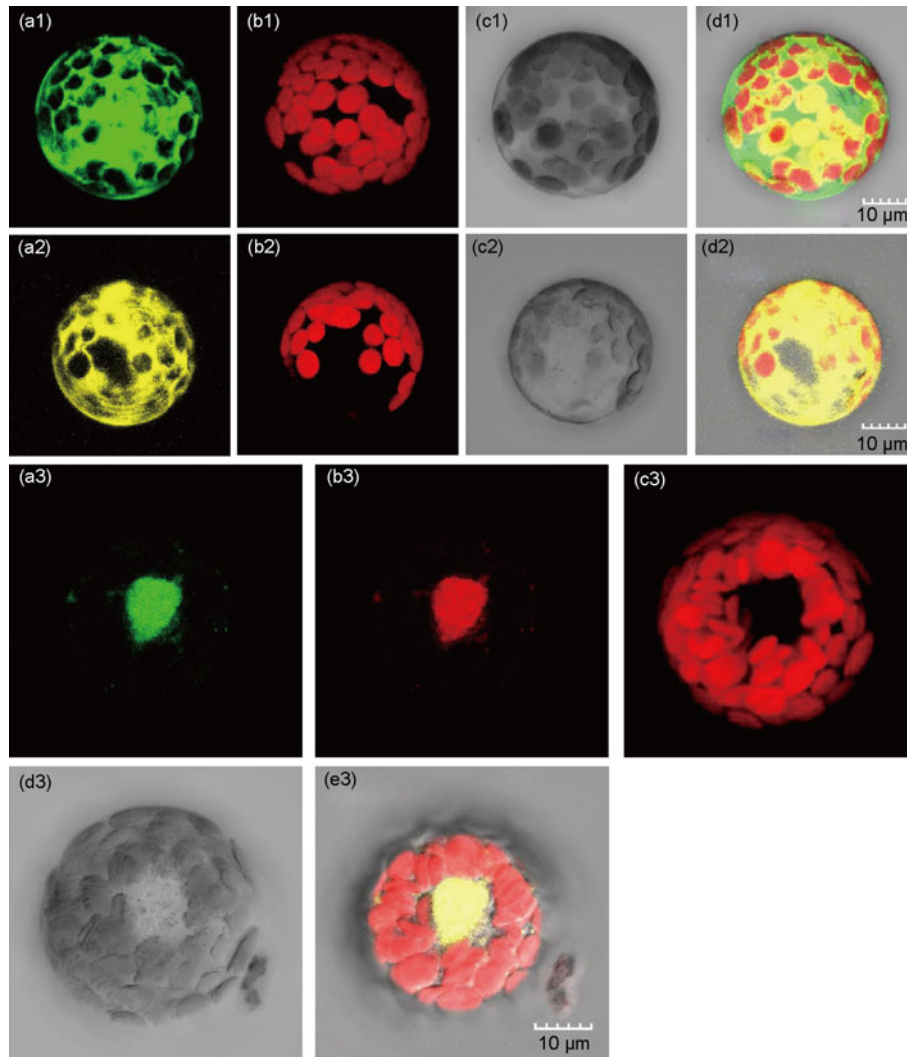


**Figure 4** Subcellular localization of BGLU10 in protoplasts. (a1)–(d1) Green fluorescent protein alone was localized throughout cells when they were transformed with pHBT-GFP vector control; (a2)–(d2) red fluorescent protein alone was localized throughout the cells when they were transformed with pHBT-DsRed vector control; (a3) green fluorescence of BGLU10::GFP fusion protein; (b3) red fluorescence of  $\gamma$ -TIP1::RFP fusion protein; (c3) autofluorescence of chloroplast; (d3) transmitted field of protoplast; (e3) merged image of (a3), (b3), (c3) and (d3).

zation suggests that ABA-GE stored in the vacuole could be hydrolyzed to release bioactive free ABA, thus increasing concentrations of active ABA.

### 2.5 *BGLU10* is induced by different abiotic stresses, and expressed in various tissues

We conducted detailed analyses of *BGLU10* expression by fusing the *BGLU10* putative promoter region to the  $\beta$ -glucuronidase (GUS) reporter. GUS staining analysis of organ-specific expression of *BGLU10* showed that this gene was transcribed in various organs, including roots, stems, leaves, flowers, and siliques, especially in mature conducting tissues (Figure 5(a)). RT-PCR analysis of the mRNAs in the detached organs of roots, leaves, stems, and flowers confirmed the results of GUS staining (Figure 5(b)). In addition, *BGLU10* was induced by ABA, salt, and drought

stresses (Figure 5(c)), suggesting that the  $\beta$ -glucosidase BGLU10 may be involved in variety of stresses and in the hydrolysis of ABA-GE, producing free ABA during plant stress responses.

## 3 Discussion

The hormone abscisic acid (ABA) regulates the development and survival of plants in response to environmental stresses. The level of ABA in plant tissues is not only controlled via its biosynthetic rate, but also by the rate of its catabolism [6]. It has long been thought that ABA-GE is the only non-active storage form of ABA [34]. In 2006, Lee et al. [17] first reported that the T-DNA insertion mutant *atbg1*, a member of  $\beta$ -glucosidase family in *Arabidopsis*, was sensitive to drought stress, and exogenously applied ABA

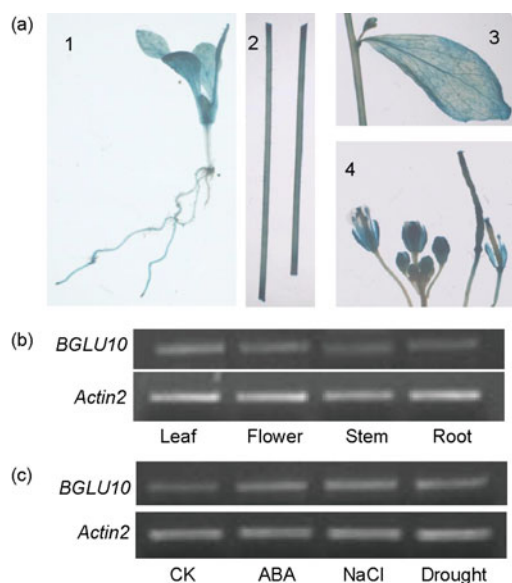


**Figure 5** Expression of *BGLU10*. (a) *BGLU10* promoter-GUS analysis of tissue expression patterns: 2-week-old plant (1), stems (2), cauline leaves (3), inflorescence and siliques (4); (b) reverse transcriptase-PCR analysis of *BGLU10* expression in various tissues; (c) reverse transcriptase-PCR analysis of *BGLU10* expression induced by abiotic stresses.

partly restored the normal phenotype. This work indicated that there is another way of producing bioactive ABA in response to dehydration stress in plants.

In this study, our data provide genetic evidence that *BGLU10* also plays a significant role in drought resistance in *Arabidopsis*. The T-DNA insertion homozygous mutant *bglu10* showed faster wilting and death than the WT under drought stress (Figure 1(c) and (d)). Infrared thermography imaging analysis (Figure 1(e)) showed that stomata of *bglu10* tended to retain a larger aperture than those of the WT, which led to greater water loss (Figure 1(g) and (h)). By contrast, the lines overexpressing *BGLU10* were more drought tolerant than the WT (Figure 2(b)–(d)). Determination of ABA content in plants under both normal watering and drought conditions showed that *BGLU10-OE* lines contained higher ABA levels than the WT, but the ABA content in *bglu10* was slightly lower than in the WT (Figure 3 (b)). Research has established that the ABA-mediated response to water deficit and osmotic stress conditions is associated with the transcriptional up-regulation of specific genes. Transcripts of *ATHB6* are upregulated in response to limited water supply, osmotic stress, and exogenous ABA [35]. The expression of *RD22*, a dehydration-responsive gene, was induced by the application of exogenous ABA and drought stress in *Arabidopsis* [30,36]. In the present work, the expressions of the marker genes *ATHB6* and *RD22* were induced by dehydration stress; their expressions were highest in *BGLU10-OE* lines and lowest in the *bglu10* mutant (Figure 3(c) and (d)). Furthermore, the total  $\beta$ -glucosidase activity was positively correlated with drought resistance in the *bglu10* mutant, WT, and *BGLU10-OE*

plants (Figure 3(a)). In addition, *BGLU10* was transcribed in various organs, including roots, stems, leaves, flowers, and siliques, especially in mature conducting tissues (Figure 5(a) and (b)), and was induced by ABA, salt, and drought (Figure 5(c)). These results are also helpful to explain the relationship between ABA content and drought tolerance, and suggest that *BGLU10*, like *ATBG1*, may function to hydrolyze ABA-GE and release free ABA to enhance the stress tolerance of plants.

In plants, ABA-GE is located in intracellular storage organelles (vacuoles), in xylem sap, and probably in the cytosol and cell wall as well [18]. Lee et al. [17] showed that the *AtBG1*  $\beta$ -glucosidase was located in the endoplasmic reticulum (ER) and remained in the ER during stress responses. Thus, the authors hypothesized that dehydration stress acts as a signal to transport ABA-GE stored in the vacuole or apoplasmic space to the ER. However, the transport systems involved in the movement of ABA-GE have not been identified yet. By using fluorescence co-localization of *BGLU10-GFP* and  $\gamma$ -TIP1-RFP transiently expressed in mesophyll protoplasts, we observed that *BGLU10* was localized in the vacuole (Figure 4 (a3) – (e3)). This result validates the predictions based on bioinformatics analyses in previous reports [19]. More importantly, the vacuolar localization of *BGLU10* suggests that it is in a position to hydrolyze ABA-GE and produce free ABA directly, without transportation. Admittedly, our results raise some new questions; for example, is ABA-GE constantly hydrolyzed to release free ABA within the vacuole, or is it rapidly hydrolyzed at particular growth stages or under specific stress conditions? What is the signal that triggers the enzymatic function of *BGLU10*? In addition, it will be interesting to determine the mechanism by which *BGLU10* is activated under abiotic stress conditions.

We thank Professor XIAO LiangTao of Hunan Agricultural University for help with ABA analyses. This work was supported by the National Natural Science Foundation of China (90817106, 31170253 and 30800075).

- 1 Finkelstein R R, Gampala S S L, Rock C D. Abscisic acid signaling in seeds and seedlings. *Plant Cell*, 2002, 14(Suppl): S15–S45
- 2 Christmann A, Moes D, Himmelbach A, et al. Integration of abscisic acid signalling into plant responses. *Plant Biol (Stuttg)*, 2006, 8: 314–325
- 3 Seki M, Umezawa T, Urano K, et al. Regulatory metabolic networks in drought stress responses. *Curr Opin Plant Biol*, 2007, 10: 296–302
- 4 Ali-Rachedi S, Boinot D, Wagner M H, et al. Changes in endogenous abscisic acid levels during dormancy release and maintenance of mature seeds: studies with the Cape Verde Islands ecotype, the dormant model of *Arabidopsis thaliana*. *Planta*, 2004, 219: 479–499
- 5 Chiwocha S D, Cutler A J, Abrams S R, et al. The *etr1-2* mutation in *Arabidopsis thaliana* affects the abscisic acid, auxin, cytokinin and gibberellin metabolic pathways during maintenance of seed dormancy, moist-chilling and germination. *Plant J*, 2005, 42: 35–48
- 6 Nambara E, Marion-Poll A. ABA biosynthesis and catabolism. *Annu Rev Plant Biol*, 2005, 56: 165–185
- 7 Wasilewska A, Vlad F, Sirichandra C, et al. An update on abscisic acid signaling in plants and more.... *Mol Plant*, 2008, 1: 198–217



- 8 Hey S J, Byrne E, Halford N G. The interface between metabolic and stress signalling. *Ann Bot*, 2010, 105: 197–203
- 9 Shinozaki K, Yamaguchi-Shinozaki K. Gene networks involved in drought stress response and tolerance. *J Exp Bot*, 2007, 58: 221–227
- 10 Urano K, Maruyama K, Ogata Y, et al. Characterization of the ABA-regulated global responses to dehydration in *Arabidopsis* by metabolomics. *Plant J*, 2009, 57: 1065–1078
- 11 Umezawa T, Okamoto M, Kushiro T, et al. CYP707A3, a major ABA 8'-hydroxylase involved in dehydration and rehydration response in *Arabidopsis thaliana*. *Plant J*, 2006, 46: 171–182
- 12 Cutler A J, Krochko J E. Formation and breakdown of ABA. *Trends Plant Sci*, 1999, 4: 472–478
- 13 Priest D M, Ambrose S J, Vaistij F E, et al. Use of the glucosyltransferase UGT71B6 to disturb abscisic acid homeostasis in *Arabidopsis thaliana*. *Plant J*, 2006, 46: 492–502
- 14 Lehmann H, Glund K. Abscisic acid metabolism-vascular/extravascular distribution of metabolites. *Planta*, 1986, 168: 559–562
- 15 Sauter A, Dietz K J, Hartung W. A possible stress physiological role of abscisic acid conjugates in root-to-shoot signalling. *Plant Cell Environ*, 2002, 25: 223–228
- 16 Kato-Noguchi H, Tanaka Y. Effect of ABA-beta-D-glucopyranosyl ester and activity of ABA-beta-D-glucosidase in *Arabidopsis thaliana*. *J Plant Physiol*, 2008, 165: 788–790
- 17 Lee K H, Piao H L, Kim H Y, et al. Activation of glucosidase via stress-induced polymerization rapidly increases active pools of abscisic acid. *Cell*, 2006, 126: 1109–1120
- 18 Dietz K J, Sauter A, Wichert K, et al. Extracellular  $\beta$ -glucosidase activity in barley involved in the hydrolysis of ABA glucose conjugate in leaves. *J Exp Bot*, 2000, 51: 937–944
- 19 Xu Z, Escamilla-Treviño L, Zeng L, et al. Functional genomic analysis of *Arabidopsis thaliana* glycoside hydrolase family 1. *Plant Mol Biol*, 2004, 55: 343–367
- 20 Yoo S D, Cho Y H, Sheen J. *Arabidopsis* mesophyll protoplasts: a versatile cell system for transient gene expression analysis. *Nat Protoc*, 2007, 2: 1565–1572
- 21 Merlot S, Mustilli A C, Genty B, et al. Use of infrared thermal imaging to isolate *Arabidopsis* mutants defective in stomatal regulation. *Plant J*, 2002, 30: 601–609
- 22 Browning G, Wignall T A. Identification and quantitation of indole-3-acetic and abscisic acids in the cambial region of *Quercus robur* by combined gas chromatography-mass spectrometry. *Tree Physiol*, 1987, 3: 235–246
- 23 Qi Q, Rose P A, Abrams G D, et al. (+)-Abscisic acid metabolism, 3-ketoacyl-coenzyme A synthase gene expression, and very-long-chain monounsaturated fatty acid biosynthesis in *Brassica napus* embryos. *Plant Physiol*, 1998, 117: 979–987
- 24 Kamboj K S, Browning G, Blake P S, et al. GC-MS-SIM analysis of abscisic acid and indole-3-acetic acid in shoot bark of apple rootstocks. *Plant Growth Regul*, 1999, 28: 21–27
- 25 Kang D J, Seo Y J, Lee J D, et al. Jasmonic acid differentially affects growth, ion uptake and abscisic acid concentration in salt-tolerant and salt-sensitive rice cultivars. *J Agron Crop Sci*, 2005, 191: 273–282
- 26 Seo H S, Kim S K, Jang S W, et al. Effect of jasmonic acid on endogenous gibberellins and abscisic acid in rice under NaCl stress. *Biol Plant*, 2005, 49: 447–450
- 27 Alonso J M, Stepanova A N, Leisse T J, et al. Genome-wide insertional mutagenesis of *Arabidopsis thaliana*. *Science*, 2003, 301: 653–657
- 28 Iuchi S, Kobayashi M, Taji T, et al. Regulation of drought tolerance by gene manipulation of 9-cis-epoxycarotenoid, a key enzyme in abscisic acid biosynthesis in *Arabidopsis*. *Plant J*, 2001, 27: 325–333
- 29 Ni F T, Chu L Y, Shao H B, et al. Gene expression and regulation of higher plants under soil water stress. *Curr Genomics*, 2009, 10: 269–280
- 30 Abe H, Yamaguchi-Shinozaki K, Urao T, et al. Role of *Arabidopsis* MYC and MYB homologs in drought- and abscisic acid-regulated gene expression. *Plant Cell*, 1997, 9: 1859–1868
- 31 Söderman E, Hjällström M, Fahleson J, et al. The HD-Zip gene ATHB6 in *Arabidopsis* is expressed in developing leaves, roots and carpels and up-regulated by water deficit conditions. *Plant Mol Biol*, 1999, 40: 1073–1083
- 32 Uno Y, Furihata T, Abe H, Yoshida R, et al. *Arabidopsis* basic leucine zipper transcription factors involved in an abscisic acid-dependent signal transduction pathway under drought and high-salinity conditions. *Proc Natl Acad Sci USA*, 2000, 97: 11632–11637
- 33 Hunter P R, Craddock C P, Di Benedetto S, et al. Fluorescent reporter proteins for the tonoplast and the vacuolar lumen identify a single vacuolar compartment in *Arabidopsis* cells. *Plant Physiol*, 2007, 145: 1371–1382
- 34 Hartung W, Sauter A, Hose E. Abscisic acid in the xylem: Where does it come from, where does it go to? *J Exp Bot*, 2002, 53: 27–32
- 35 Deng X, Phillips J, Bräutigam A, et al. A homeodomain leucine zipper gene from *Craterostigma plantagineum* regulates abscisic acid responsive gene expression and physiological responses. *Plant Mol Biol*, 2006, 61: 469–489
- 36 Yamaguchi-Shinozaki K, Shinozaki K. The plant hormone abscisic acid mediates the drought-induced expression but not the seed-specific expression of *rd22*, a gene responsive to dehydration stress in *Arabidopsis thaliana*. *Mol Gen Genet*, 1993, 238: 17–25

**Open Access** This article is distributed under the terms of the Creative Commons Attribution License which permits any use, distribution, and reproduction in any medium, provided the original author(s) and source are credited.